https://doi.org/10.5194/egusphere-2024-4013
Preprint. Discussion started: 9 January 2025

Human Activities Caused Hypoxia Expansion in a Large Eutrophic Estuary: Non-negligible Role of Riverine Suspended Sediments

Yue Nan[1], Zheng Chen[2], Bin Wang[3], Bo Liang[4], Jiatang Hu[1,5,6*]

[1] School of Environmental Science and Engineering, Sun Yat-Sen University, Guangzhou, 510275, China

[2] Earth, Ocean and Atmospheric Sciences Thrust, The Hong Kong University of Science and Technology (Guangzhou), Guangzhou, 511455, China

[3] Department of Oceanography, Dalhousie University, Halifax, Nova Scotia, Canada

[4] Eco-Environmental Monitoring and Research Center, Pearl River Valley and South China Sea Ecology and Environment Administration, Ministry of Ecology and Environment of the People's Republic of China, Guangzhou, 510611, China

[5] Guangdong Provincial Key Laboratory of Environmental Pollution Control and Remediation Technology, Guangzhou, 510275, China

[6] Southern Marine Science and Engineering Guangdong Laboratory (Zhuhai), Zhuhai, 519000, China

Correspondence: Jiatang Hu (hujtang@mail.sysu.edu.cn)

https://doi.org/10.5194/egusphere-2024-4013
Preprint. Discussion started: 9 January 2025

Abstract

Increase in riverine nutrient loads was generally recognized as the primary cause of coastal deoxygenation, whereas the role of other riverine factors, especially suspended sediments, has received less attention. This study aims to discern the impacts of anthropogenic alterations in various riverine inputs on the subsurface deoxygenation over the past three decades in a large river-dominated estuary, the Pearl River Estuary (PRE). By utilizing the physical-biogeochemical model, we reproduced the observed dissolved oxygen (DO) conditions off the PRE in the historical period (the 1990s with high-suspended sediments-DO and low-nutrient inputs) and the present period (the 2010s with low-suspended sediments-DO and high-nutrient inputs). Due to the decadal changes in riverine inputs, the PRE has witnessed more extensive and persistent low-oxygen events during summer in the 2020s, with larger spatial extents of ~2926 km^2 for low oxygen (DO < 4 mg/L, increased by ~148% relative to the 1990s) and 617 km^2 for hypoxia (DO < 3 mg/L, by 192%) and longer duration (by ~15-35 days), evolving into three distinct hypoxic centers controlled by different factors. Model experiments suggested that the decreased riverine DO content (46%) has led to a low-oxygen expansion in the upper regions, accounting for 44% to the total increment. Meanwhile, the increased nutrient levels (100% in nitrogen and 225% in phosphorus) and the declined suspended sediment concentration (60%) have jointly promoted the primary production and bottom oxygen consumptions (dominated by sediment oxygen uptake), thus resulting in a substantial enlargement of low-oxygen area (104%) and hypoxic area (192%) in the lower reaches. Our results revealed a more critical role of the riverine suspended sediment decline in the exacerbation of eutrophication and deoxygenation off the PRE via improving light conditions to support higher local productivity, which could further amplify the effect combined with the growth in nutrients and confound the effectiveness of hypoxia mitigation under nutrient controls. Overall, in the context of global changes in riverine suspended sediments, it is imperative to reassess the contribution of riverine inputs to the coastal deoxygenation worldwide over the past

https://doi.org/10.5194/egusphere-2024-4013
Preprint. Discussion started: 9 January 2025

decades, given that the impact of suspended sediments has been constantly overlooked in relevant investigations.

Key words: Deoxygenation; suspended sediments; nutrient inputs; decadal changes; Pearl River Estuary

Graphical Abstract

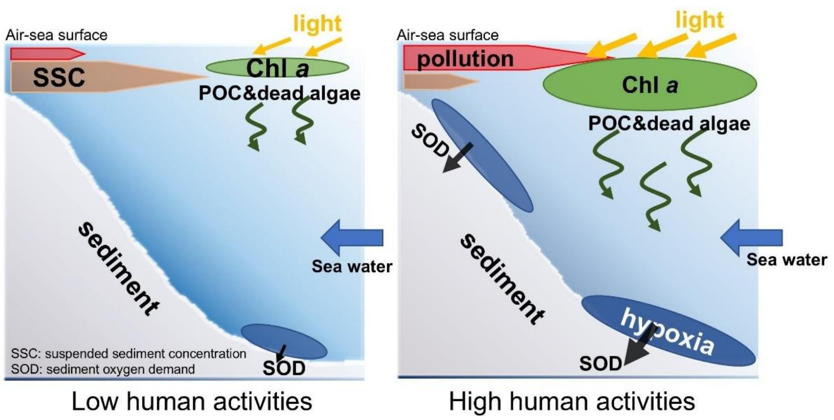

DO process under low human activities (left) and high human activities (right). Note that pollution indicates DIN, DIP and low oxygen water from the discharge.

1. Introduction

Hypoxia emerges when dissolved oxygen (DO) concentration drops below 3 mg/L in aquatic systems. It is an undesirable phenomenon which can lead to a series of biological and ecological consequences, such as damaging the habitat for aquatic organisms and imposing detrimental effects on the ecosystem community structure (Diaz and Rosenberg, 2008; Roman et al., 2019). Due to the substantial impacts from human socioeconomic activities, coastal regions have become a hotspot for hypoxia (Breitburg et al., 2018; Pitcher et al., 2021). Moreover, long-term exacerbation of hypoxia with spatial expansion and increased intensity has been frequently reported in estuarine and coastal regions worldwide during the past decades, including the Baltic

https://doi.org/10.5194/egusphere-2024-4013
Preprint. Discussion started: 9 January 2025

Sea (Carstensen et al., 2014), the northern Gulf of Mexico (Bianchi et al., 2010), Chesapeake Bay (Murphy et al., 2011), the Yangtze River Estuary (Chen et al., 2017), and the Pearl River Estuary (Hu et al., 2021).

Plenty of studies were conducted to reveal the mechanism of hypoxia formation and evolution in coastal regions. It has been widely recognized that coastal deoxygenation is largely attributed to the eutrophication-driven production of organic matters (Su et al., 2017; Wang et al., 2016), which sink to the subsurface waters and bottom sediments, leading to intense oxygen depletion (Wang et al., 2014). This would induce hypoxia when the density stratification restricts DO replenishment from the surface waters (Wang et al., 2018). One important reason underlying eutrophication and hypoxia is the excessive nutrients that are discharged into the water column and stimulate phytoplankton blooms (Cullen, 2015; Wang et al., 2016; Wang et al., 2021). In addition, an improved light condition, e.g., due to the decreased suspended sediment loads, could also favor the enhancement of local production and hence hypoxia (Ge et al., 2020; Huang et al., 2022). The effects of nutrient and light conditions vary in coastal systems due to different hydrodynamic and topographic features, which makes the formulation of hypoxia mitigation strategies more challenging. Therefore, a quantitative assessment on the importance of these factors in generating hypoxia is crucial for understanding the primary drivers of hypoxia evolution and for proposing effective countermeasures.

A case in point is the Pearl River Estuary (PRE), which is situated in the northern South China Sea and close to the Guangdong-Hong Kong-Macao Great Bay Area (Fig. 1a). Owing to the relatively large nutrient inputs and vertical stratification formed by freshwater plume, hypoxia typically occurs during summer in the bottom waters of the PRE. Before the 2000s, it was an episodic and small-scale issue because of the synergetic effect of shallow topography, high turbidity (Ma et al., 2022), and the intermittent stratification due to periodic disturbance by the tides. However, large-scale occurrences of low oxygen (when DO < 4 mg/L) and hypoxia were frequently reported

https://doi.org/10.5194/egusphere-2024-4013
Preprint. Discussion started: 9 January 2025

in recent years. For example, it was estimated that the low-oxygen area within the PRE achieved 1000 km^2 and 1500 km^2 during summer in 2010 (Wen et al., 2020) and 2015 (Li et al., 2018), respectively, which were nearly double to that before the 2000s (Li et al., 2020b). Hu et al. (2021) compiled historical observations over four decades to investigate the long-term deoxygenation trend and its spatial expansion in the PRE. They highlighted the significant contributions of increased nutrient and decreased sediment fluxes from the Pearl River to the exacerbation of low-oxygen conditions in the region. Besides, the low-oxygen inflows from the Pearl River could also contribute to the low-oxygen area in the upper estuary (Hu et al., 2021). Nevertheless, a quantitative understanding of their relative contributions to the low-oxygen expansion in the PRE is lacking, particularly in different subregions (Fig.1b) where the mechanisms controlling the low-oxygen conditions are different (Li et al., 2020a).

In this study, we use a coupled physical-biogeochemical model to investigate the decadal changes (the 1990s versus the 2010s) in summertime DO contents and related biogeochemical processes in the PRE and to quantify the relative contributions of the changing riverine inputs (including nutrients, suspended sediments, and oxygen content; Fig. 1c-f) to the long-term expansion of low oxygen (DO < 4 mg/L) and hypoxia (DO < 3 mg/L) in the region.

2. Material and methods

2.1 Study area

The PRE and its adjacent shelf waters (Fig. 1a) represent an estuarine system under intensive human activities. One major anthropogenic impact in the PRE is the terrestrial substances fed by the Pearl River, which is the third largest river in China with an average annual runoff of 3.26×10^8 m^3 (Luo et al., 2002), through eight river outlets, including Humen, Jiaomen, Hongqili, Hengmen, Modaomen, Jitimen, Hutiaomen, and Yamen (Fig. 1a). The long-term DO and water quality data used here were collected from open sources (e.g. government websites) and published studies

https://doi.org/10.5194/egusphere-2024-4013
Preprint. Discussion started: 9 January 2025

(Table S1). Over the past few decades, the terrestrial inputs from the Pearl River has experienced remarkable changes in oxygen content, sediment loads, and nutrients including dissolved inorganic nitrogen (DIN) and dissolved inorganic phosphorus (DIP) (Fig. 1c-f). Consequently, the ecological environments of the PRE have changed significantly.

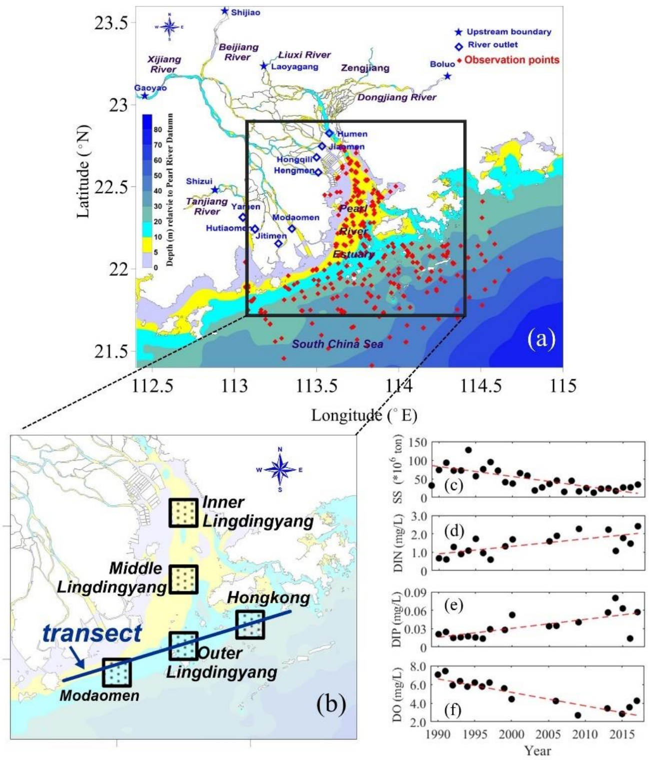

Fig. 1. (a) Study area of the PRE and sampling sites during 1985-2017; (b) five subregions and a transect along the coastal transition zone used for analysis; (c) annual loads of suspended sediments (SS) from the Pearl River; (d-f) the summertime concentrations of nutrients (DIN, DIP) and dissolved oxygen (DO) in the river outlets of the PRE.

In the 1990s, the PRE displayed a low level of eutrophication due to the weak urbanization in the upstream regions and high turbidity because of the absence of large-scale hydraulic facilities, e.g., dams, which could block the suspended sediments from being transported into the estuary. Until the late 1990s, at least 8636 reservoirs were

https://doi.org/10.5194/egusphere-2024-4013
Preprint. Discussion started: 9 January 2025

established in the Pearl River basin, the vast majority of which were built after China's reform and opening up in 1980 (Wu et al., 2016). After the 2000s, with the acceleration of urbanization and construction of hydraulic facilities, the PRE has undergone a significant increase in nutrients and decline in sediment loads (Fig. 1c-e), both of which are favorable for phytoplankton blooms and therefore for eutrophication and hypoxia. These long-term variations of riverine substances have also been reported by Lai et al. (2022) and Hu et al. (2021). In the meantime, the oxygen content in the PRE has exhibited a notable drawdown with significant expansions in low-oxygen extents in recent summers (Fig. 2), which has been revealed by the cruise observations in the PRE (Li et al., 2021; Su et al., 2017; Hu et al., 2021; Lu et al., 2018).

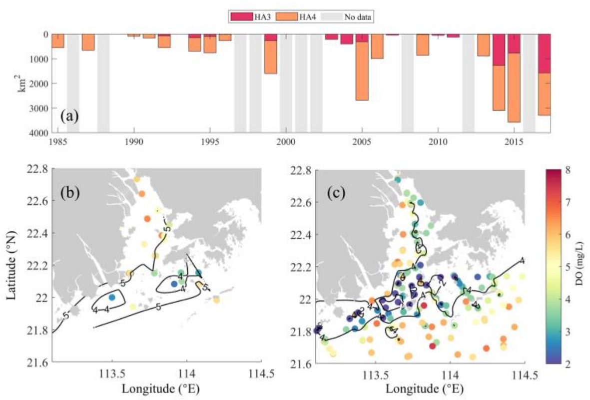

Fig. 2. (a) Interannual variations of low-oxygen area (HA4, DO < 4 mg/L) and hypoxic area (HA3, DO < 3 mg/L) in the bottom waters of the PRE during summer estimated from the cruise observations (note that the grey patches represent the lack of data); spatial distributions of summer-averaged DO concentrations during (b) 1991-1996 and (c) 2013-2017.

2.2 Model settings and validation

2.2.1 Model descriptions and settings

A 1D-3D coupled physical-biogeochemical model, which has been extensively verified and applied in the PRE (Wang et al., 2017; Wang et al., 2018; Hu et al., 2011; Zhang et al., 2022), was utilized here to reproduce the oxygen dynamics under the long-term changes in riverine nutrients, suspended sediment concentration (SSC), and

https://doi.org/10.5194/egusphere-2024-4013
Preprint. Discussion started: 9 January 2025

oxygen content (Fig. 1c-f). For the sake of conciseness in the main text, detailed descriptions on the physical and suspended sediment modules were provided in the Supplement (Text S1). Regarding the biogeochemical module, it is based on the Row-Column Aesop (RCA), which simulates interactive cycles of oxygen, carbon, nitrogen, phosphorus, and silicon in the water column (Fizpartick, 2004). As for the oxygen dynamics, it can be described as follows:

$$\frac{\partial DO}{\partial t} = -\left(u\frac{\partial DO}{\partial x} + v\frac{\partial DO}{\partial y} + w\frac{\partial DO}{\partial z}\right) + \frac{\partial}{\partial x}\left(A_H\frac{\partial DO}{\partial x}\right) + \frac{\partial}{\partial y}\left(A_H\frac{\partial DO}{\partial y}\right) + \frac{\partial}{\partial z}\left(K_H\frac{\partial DO}{\partial z}\right) + Rea + Phot + WCR + SOD \quad (1)$$

where DO represents the dissolved oxygen concentration (mg/L); $-\left(u\frac{\partial DO}{\partial x} + v\frac{\partial DO}{\partial y} + w\frac{\partial DO}{\partial z}\right)$ represents the horizontal and vertical advection of oxygen (mg O_2 L^{-1} day^{-1}); $\frac{\partial}{\partial x}\left(A_H\frac{\partial DO}{\partial x}\right) + \frac{\partial}{\partial y}\left(A_H\frac{\partial DO}{\partial y}\right) + \frac{\partial}{\partial z}\left(K_H\frac{\partial DO}{\partial z}\right)$ represents the horizontal and vertical diffusion of oxygen (mg O_2 L^{-1} day^{-1}); Rea and $Phot$, WCR, and SOD represent the rates of air-water oxygen exchange, photosynthesis, water column respiration, and sediment oxygen demand, respectively (unit: mg O_2 L^{-1} day^{-1}). The SOD is calculated by the sediment flux module (SFM) coupled to the RCA. The sediment module simulates the sedimentation and remineralization of organic carbon, nitrogen, and phosphorus, and dynamically estimates the oxygen and nutrient fluxes across the sediment-water interface (Fizpartick, 2004).

The growth of phytoplankton is co-limited by temperature, light, and nutrient conditions. The calculation of gross primary production (GPP, mg C L^{-1} day^{-1}) of phytoplankton in RCA (Fizpartick, 2004) is determined as:

$$GPP = G_{Pmax} * e^{-\beta(T_{opt}-T)^2} * G_N(N) * G_I(I) * P_c \quad (2)$$

where G_{Pmax} is the maximum grow rate of phytoplankton at the optimum temperature (day^{-1}); T_{opt} is the optimum temperature (°C); β is the shaping coefficients; T is the water temperature (°C); $G_I(I)$ is the light limitation factor; $G_N(N)$ is the nutrient limitation factor; P_c is the phytoplankton biomass (mg C L^{-1}).

The nutrient limitation factor is parameterized as:

https://doi.org/10.5194/egusphere-2024-4013
Preprint. Discussion started: 9 January 2025

$$G_N(N) = Min\left(\frac{DIN}{K_{mN}+DIN}, \frac{DIP}{K_{mP}+DIP}, \frac{Si}{K_{mSi}+Si}\right) \tag{3}$$

where DIN, DIP, and Si represent the concentration (mg L^{-1}) of dissolve inorganic nitrogen (including NO_3^- and NH_4^+), dissolve inorganic phosphorus (PO_4^{3-}), and dissolve inorganic silicon (SiO_3^{2-}), respectively; K_{mN}, K_{mP}, and K_{mSi} represent the half-saturation constants (mg L^{-1}) for DIN, DIP, and Si, respectively. It should be noted that a higher nutrient limitation factor $G_N(N)$ indicates a weaker nutrient limitation effect on phytoplankton growth (Fizpartick, 2004). Moreover, the nitrogen and phosphorus limitation are more significant than silicon limitation within the PRE, thus this study mainly focuses on the former.

The light limitation factor $G_I(I)$ is parameterized as:

$$G_I(I) = \frac{e}{k_eH}[\exp\left(\frac{-I_0(t)}{I_s}e^{-k_eH}\right) - exp\frac{-I_0(t)}{I_s}] \tag{4}$$

$$k_e = k_{ebase} + k_c * a_{cchl} * P_c + k_{sed} * SSC \tag{5}$$

$$I_0 = I_{surf} * e^{-k_e*H} \tag{6}$$

where H is the depth of water column (m); I_0 is the incident light intensity at the segment surface (ly day^{-1}); I_s is the saturating light intensity (ly day^{-1}); k_e is the light extinction coefficient (m^{-1}); k_{ebase} is the background light extinction coefficient of water (m^{-1}); k_c is the phytoplankton-related extinction coefficient (m^2 mg^{-1} Chla); a_{cchl} is the ratio of chlorophyll to phytoplankton carbon biomass; k_{sed} is the SSC-related extinction coefficient (m^2 mg^{-1} SSC); I_{surf} is the instant light radiation received at the water surface (ly day^{-1}) (Fizpartick, 2004; Zhang and Li, 2010).

To estimate the spatial characteristics of light conditions, we also calculated the eutrophic depth in the PRE, which is defined as the water depth reached by 1% of the surface light intensity (I_0). Basically, a larger eutrophic depth indicates a better light condition for phytoplankton growth.

2.2.2 Model validation

The coupled physical-biogeochemical model mentioned above has already been validated against a variety of observations for several periods, which showed good

https://doi.org/10.5194/egusphere-2024-4013
Preprint. Discussion started: 9 January 2025

performance in reproducing the physical conditions, suspended sediment dynamics, and biogeochemical cycles in the PRE. We briefly summarized the validation results here. For the physical and suspended sediment modules, Hu and Li (2009) has applied the 1D-3D coupled model to establish 30-day realistic simulations for July 1999 and February 2001. The simulated water levels, discharges, salinity, and SSC agreed well with the observations in the Pearl River network and the PRE for both periods, with correlation coefficients all greater than 0.65 in summer. The simulated SSC at the surface was also compared to satellite remote sensing data, which showed a fairly close spatial pattern and comparable concentration magnitude. Furthermore, Wang et al. (2017) provided an extensive model validation using field data collected from four seasonal cruises in 2006, with high correlations for water levels (> 0.95), salinity (> 0.90) and temperature (> 0.80) and low root-mean-standard-errors between the simulation and observations in summer.

Then, the biogeochemical module was established and used to explore the nutrient and oxygen dynamics off the PRE in July 1999 and January-December 2006 (Hu and Li, 2009; Wang et al., 2017). The point-to-point comparisons with the water quality profiles indicated that the biogeochemical module was robust to reproduce the spatial distributions of ammonia, nitrate, phosphorus, oxygen, and chlorophyll *a* in the PRE. In addition, Wang et al. (2017) has compared the simulated oxygen kinetic terms (including the air-sea re-aeration rate, water-column respiration and production rates, and sediment oxygen demand) with observations in summer, which demonstrated the model's capability in representing the important oxygen source-sink processes (e.g., oxygen consumptions across the sediment-water interface) in the PRE. Detailed model settings and parameters can be found in Wang et al. (2017).

2.3 Model experiments

Based on the well-validated model run in 2006 (Wang et al., 2017), the present study performed diagnostic simulations for two representative periods, characterized

https://doi.org/10.5194/egusphere-2024-4013
Preprint. Discussion started: 9 January 2025

by low nutrients and high suspended sediments and oxygen content during 1991-1996 (referring as to the "1990s case"; Table 1) versus high nutrients and low suspended sediments and oxygen content during 2013-2017 (referring as to the "2010s case"). Each case was run from 1 January to 31 August, driven by climatological physical conditions (freshwater discharges and wind speeds) averaged over 1990-2017 and by mean observed values of riverine water quality components in the corresponding period. Specifically in summertime (a period used for formal analysis here), the riverine concentrations were set to 1.0 mg/L (DIN), 0.02 mg/L (DIP), and 6.5 mg/L (DO) in the 1990s case, while they were set to 2.0 mg/L, 0.065 mg/L, and 3.5 mg/L in the 2010s case (Table 1). The riverine SSC was specified at 40 mg/L in the 2010s according to the in-situ observation near the Humen outlet in 2015 summer (Chen et al., 2020), and was set to 100 mg/L in the 1990s based on the ratio of the sediment loads between the 1990s and the 2010s (2.5 times). Furthermore, three additional model scenario simulations were conducted in order to disentangle the individual impact of each varying riverine input on the summer deoxygenation off the PRE. The setting of each scenario was identical to that of the 1990s case except that the riverine nutrients, SSC, and DO were separately replaced by the representative value in the 2010s (referring as to the "High-nutrient case", "Low-SSC case", and "DO-restore case", respectively; Table 1).

Table 1. Riverine inputs (in unit of mg L^{-1}) for model experiments.

Cases	DIN	DIP	DO	SSC
1990s	1.0	0.020	6.5	100
2010s	2.0	0.065	3.5	40
High-nutrient	2.0	0.065	6.5	100
Low-SSC	1.0	0.020	6.5	40
DO-restore	2.0	0.065	6.5	40

3. Results

https://doi.org/10.5194/egusphere-2024-4013
Preprint. Discussion started: 9 January 2025

3.1 Responses of eutrophication to human-induced changes in the PRE

3.1.1 Long-term variations in water quality distributions

To examine changes in eutrophication (a key process affecting DO dynamics) and its influential factors during summer in the PRE, we compared the simulated distributions of SSC, nutrients, Chl *a*, and POC in the surface waters between the 1990s and the 2010s cases (Fig. 3) as well as their vertical integrations in subregions (Table 2). Model results showed that the surface SSC within the PRE largely declined during the two periods. In the 1990s, SSC maintained at a high level in the inner Lingdingyang Bay (see its location in Fig. 1b), ranging from 70.0 to 100.0 mg/L (Fig. 3a). Due to the consecutive sinking along with water transport, SSC dropped to ~10.0 mg/L in the lower reaches of the PRE. While in the 2010s, the riverine sediment loads have remarkably decreased, resulting in a corresponding drawdown in SSC downstream (Fig. 3b-c). Overall, the vertically-integrated SSC content in the inner Lingdingyang Bay and lower PRE dropped by 56.1% and 45.6%-47.3% to 244.5 mg/m^2 and 38.4-69.2 mg/m^2, respectively (Table 2).

In terms of nutrients, the variation induced by riverine inputs was also evident during the two periods, acting on the main estuary in association with the spreading of the river plume. As shown, the DIN content in the 1990s was mostly below 1.5 mg/L within the entire PRE (Fig. 3d). With respect to the 2010s, the DIN concentration has increased by 0.8 mg/L and 0.2 mg/L in the surface waters of the upper Lingdingyang Bay and the lower PRE, respectively (Fig. 3e-f). The vertically-integrated DIN mass has increased by 41.9%-102% in the PRE (Table 2). A similar situation occurred with respect to DIP, with its content increasing from 0.04 mg/L in the 1990s to 0.07 mg/L in the 2010s in the high-DIP area adjacent to the middle Lingdingyang Bay (Fig. 3g-i). In terms of vertical integration, DIP increased by 9%-108%, with the lowest increases located in the Hong Kong waters downstream of the estuary (Table 2).

https://doi.org/10.5194/egusphere-2024-4013
Preprint. Discussion started: 9 January 2025

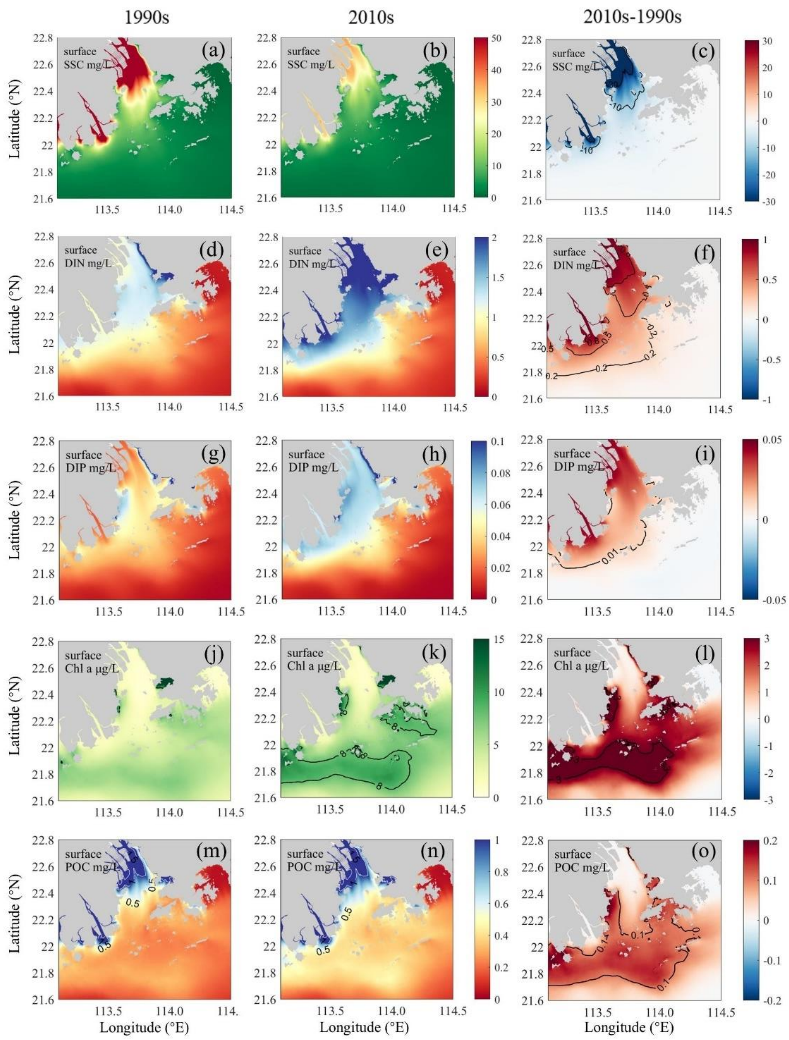

Fig. 3. Simulated distributions of (a-c) SSC, (d-f) DIN, (g-i) DIP, (j-l) Chl *a*, and (m-o) POC concentrations in the surface waters of the PRE for the 1990s (left panels) and the 2010s (middle panels) as well as their differences (right panels).

https://doi.org/10.5194/egusphere-2024-4013
Preprint. Discussion started: 9 January 2025

Table 2. Vertical integrations of DIN, DIP, SSC, Chl *a*, and POC contents; nutrient limitation index and euphotic depth; and DO concentrations, low-oxygen frequency (HF4), hypoxia frequency (HF3), and oxygen consumption rates in the bottom waters for subregions of the PRE (see locations in Fig. 1b) during the 1990s and the 2010s.

Subregions	Inner Lingdingyang Bay		Middle Lingdingyang Bay		Modaomen sub-estuary		Outer Lingdingyang Bay		Hong Kong waters	
Cases	1990s	2010s	1990s	2010s	1990s	2010s	1990s	2010s	1990s	2010s
DIN (mg m^{-2})	6.58	12.24	5.42	9.20	4.89	7.62	5.17	7.92	3.62	5.14
DIP (mg m^{-2})	0.23	0.48	0.34	0.48	0.55	0.71	0.56	0.66	0.51	0.56
Nutrient limitation index	0.94	0.97	0.95	0.97	0.92	0.94	0.91	0.93	0.83	0.85
SSC (mg m^{-2})	556.5	244.5	332.9	164.6	120.4	63.4	127.7	69.2	70.6	38.4
Euphotic depth (m)	-1.3	-2.3	-2.0	-4.2	-9.5	-11.2	-11.8	-15.2	-20.7	-21.0
Chl *a* (μg m^{-2})	5.0	7.1	11.7	22.9	39.4	70.4	40.7	72.9	74.3	108.9
POC (mg m^{-2})	8.6	8.64	4.8	5.31	4.82	6.39	5.33	6.85	6.21	7.91
Bottom DO (mg L^{-1})	4.55	3.52	4.31	3.90	3.50	2.84	4.96	4.12	4.36	3.52
HF4	25.0%	79.7%	26.8%	65.2%	84.5%	99.1%	4.5%	49.3%	20.5%	61.1%
HF3	6.5%	27.6%	4.8%	10.1%	25.2%	56.5%	3.5%	9.1%	4.8%	21.4%
WCR (mg O_2 L^{-1} day^{-1})	-0.38	-0.45	-0.20	-0.25	-0.09	-0.11	-0.07	-0.09	-0.06	-0.07
SOD (mg O_2 L^{-1} day^{-1})	-1.72	-1.62	-0.89	-0.89	-0.24	-0.46	-0.28	-1.12	-0.91	-1.48

Note: HF4 (frequency of DO < 4 mg L^{-1}); HF3 (frequency of DO < 3 mg L^{-1}).

https://doi.org/10.5194/egusphere-2024-4013
Preprint. Discussion started: 9 January 2025

In response to changes in light (affected by the SSC content) and nutrient conditions, phytoplankton biomass has substantially grown in the 2010s, indicated by the increased Chl *a* concentration. In the 1990s, the phytoplankton biomass was at a low level, with the Chl *a* generally below 8.0 μg/L in the surface waters (Fig. 3j). As for the 2010s, significant phytoplankton blooms were found along the Modaomen sub-estuary, outer Lingdingyang Bay, and Hong Kong waters (Fig. 3k-l), with the vertically-integrated Chl *a* content rising by 31.0 μg/m^2 (by 78.7% compared to the 1990s), 32.2 μg/m^2 (79.1%), and 34.6 μg/m^2 (46.6%), respectively (Table 2). As a result of the elevated primary production, a great amount of organic matter was produced in the PRE. Spatially coupled to the growth of Chl *a* (Fig. 3l), the POC content has significantly increased in the 2010s, especially in the lower PRE (Fig. 3m-o), with the vertically-integrated concentration increasing by 1.5-2.0 mg/m^2 (by 27.4%-32.6% compared to the 1990s) over the water column (Table 2).

3.1.2 Long-term variations in nutrient and light limitations

The primary production in the PRE was controlled by the synergistic effects of nutrient and light conditions. We calculated the nutrient limitation factor and the eutrophic depth to quantify the intensity of nutrient limitation and light limitation on algae growth. It should be noted that a smaller nutrient limitation index and a shallower eutrophic depth represent a stronger nutrient limitation and a stronger light limitation, respectively. Results showed that the nutrient limitation exhibited a distinct estuary-shelf gradient, in which the Hong Kong waters experienced more severe nutrient limitation than the Modaomen sub-estuary and Lingdingyang Bay (Fig. 4a, c). Specifically, the nutrient limitation index decreased from the upper estuary (0.94) to the Hong Kong waters (0.83) in the 1990s. By contrast, the light limitation has attenuated along the river plume transport, largely ascribed to the decreased SSC (Fig. 3a-b). Compared to the Hong Kong waters, the regions adjacent to river outlets underwent more severe light limitation, shown by the eutrophic depth (Fig. 4b) increasing from the Lingdingyang Bay (1.3 m) and Modaomen sub-estuary (9.5 m) to the Hong Kong

https://doi.org/10.5194/egusphere-2024-4013
Preprint. Discussion started: 9 January 2025

waters (20.7 m).

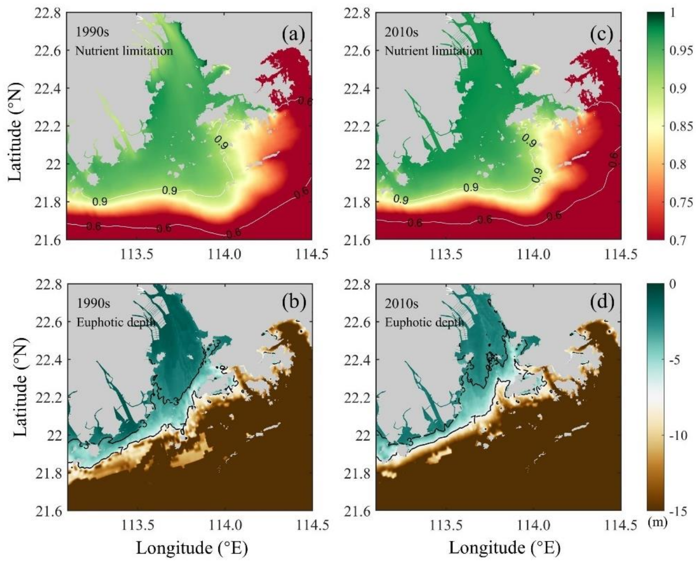

Fig. 4. Simulated distributions of (a, c) nutrient limitation index for the growth of phytoplankton and (b, d) euphotic depth (in unit of m) in the 1990s and the 2010s.

Due to the growth in nutrient loads, nutrient limitation has relieved in the 2010s. For instance, the nutrient limitation index in the Hong Kong waters has increased to 0.85 (by 2.4% of the 1990s) in the 2010s (Table 2). In comparison, the relief of light limitation was more evident with the reduced riverine suspended sediments. The deepening of the euphotic depth in the Lingdingyang Bay was significantly greater than that in the lower estuary (Fig. 4b, d). In the inner Lingdingyang and middle Lingdingyang Bays, the euphotic depth increased by 1 m and 2.2 m (by 76.9% and 110.0% relative to the 1990s, Table2), respectively. The alterations in light conditions in the remaining area were relatively minor, with the eutrophic depth increasing to 11.2 m (by 17.9%) in the Modaomen sub-estuary and to 21 m (by 1.4%) in the Hong Kong waters during the 2010s (Table 2).

https://doi.org/10.5194/egusphere-2024-4013
Preprint. Discussion started: 9 January 2025

3.2 Responses of DO dynamics to human-induced changes in the PRE

3.2.1 Variations in DO distributions and hypoxia occurrences

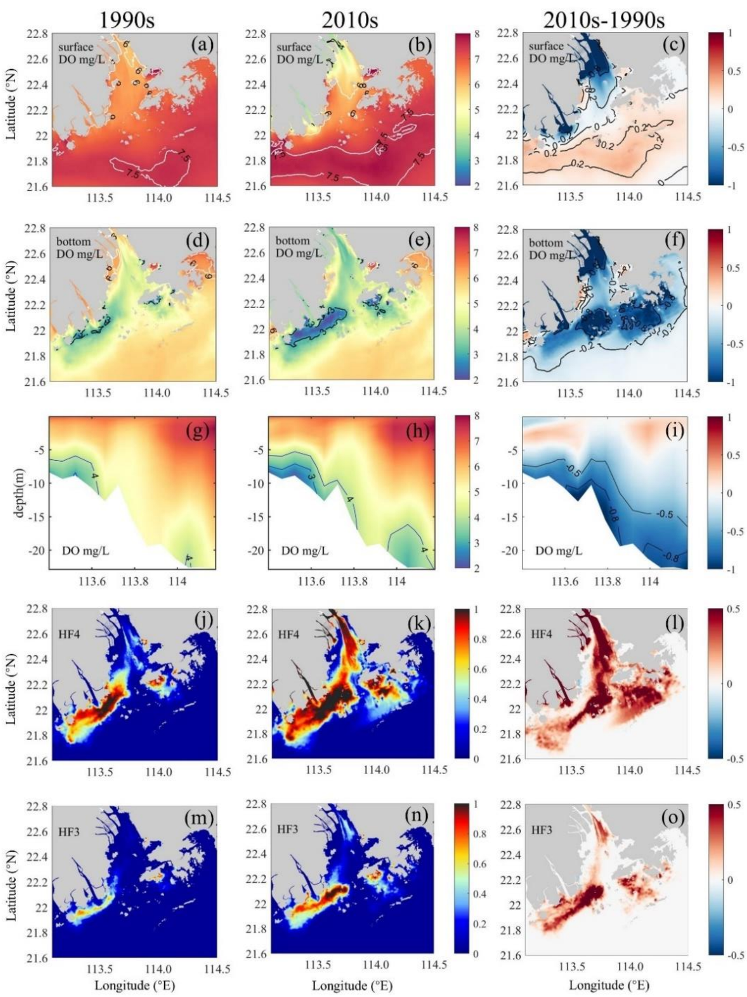

Fig. 5. (a-c) Surface DO and (d-f) bottom DO distributions, (g-i) vertical DO distributions along the transect (see its location in Fig. 1b), and (j-l) low-oxygen frequency (HF4, DO < 4 mg/L) and (m-o) hypoxia frequency (HF3, DO < 3 mg/L) in the bottom waters of the PRE for the 1990s (left panels) and the 2010s (middle panels) as well as their differences (right panels).

https://doi.org/10.5194/egusphere-2024-4013
Preprint. Discussion started: 9 January 2025

Our model results demonstrated significant changes in the spatial pattern of summertime DO and hypoxia incidences from the past to the present (Fig. 5). The surface DO concentration in the 1990s was generally higher than 6 mg/L and exhibited an increasing trend towards the shelf regions (Fig. 5a). While in the 2010s, the surface DO has undergone an evident increase by 0.2-0.3 mg/L (Fig. 5b-c), with an oxygen-enriched zone in the lower PRE, which was closely coupled to the surface high Chl *a* value (Fig. 3k). However, low-oxygen events (DO < 4 mg/L) have appeared in the surface waters adjacent to the river outlets in the 2010s (Fig. 5b) due to the low DO influx from the Pearl River along with the freshwater discharge.

In the bottom waters, the observed shift from small-scale hypoxia in the 1990s to extensive hypoxia in the 2010s (Fig. 2b-c) was well reproduced by our model (Fig. 5d-e). In the 1990s, the low-oxygen events were primarily concentrated along the western side of the PRE (i.e. the Modaomen sub-estuary and adjacent waters; Fig. 5d). The simulated low-oxygen area (HA4) and hypoxic area (HA3) were approximately 1179.7 km^2 and 211.3 km^2 (Table 3), respectively, which is consistent with the observational estimates of 802 ± 437 (mean ± standard deviation) and 131 ± 84 km^2 during the summers of 1994-1999 (Fig. 2a). The low-oxygen conditions have considerably worsened over the estuary in the 2010s (Fig. 5e-f), especially evident in the inner Lingdingyang Bay, outer Lingdingyang Bay, and Hong Kong waters. The bottom DO levels have dropped to 2.8-4.1 mg/L on average in the five subregions (Table 2). Simultaneously, the simulated low-oxygen area (HA4) has increased to ~1.5 times larger than that in the 1990s, reaching 2925.5 km^2 (Table 3). The enlarged low-oxygen coverage in our model is consistent with the observational estimates of 2715 ± 1068 km^2 during 2013-2017 (Fig. 2a). Besides, the simulated hypoxic area (HA3) has approximately increased by twofold and reached 617.2 km^2 in the 2020s, which is also comparable to the observational estimates of 901 ± 591 km^2 during 2013-2017.

https://doi.org/10.5194/egusphere-2024-4013
Preprint. Discussion started: 9 January 2025

Table 3. Simulated low-oxygen (HA4, DO < 4 mg/L) and hypoxic (HA3, DO < 3 mg/L) areas in the bottom waters of the PRE and their changes relative to the 1990s.

Cases	HA4 (km^2)	Percentage of change	HA3 (km^2)	Percentage of change
1990s	1179.7	/	211.3	/
2010s	2925.5	+148%	617.2	+192%
High-nutrient	1542.6	+31%	282.5	+34%
Low-SSC	1737.0	+47%	412.4	+95%
DO-restore	2409.7	+104%	617.2	+192%

In addition, the two observed hypoxic centers along the coastal transition zone (i.e., the Modaomen sub-estuary and Hong Kong waters; Fig. 2b-c) were also successfully reproduced by our model, showing heterogeneous deoxygenation features in terms of spatial extents and duration (Fig. 5g-o). In the 1990s, the low-oxygen conditions in these two centers were confined to a relatively small extent, especially in the Hong Kong waters, where the simulated thickness of low oxygen (DO < 4 mg/L) was less than 1 m (Fig. 5g). The low-oxygen and hypoxic waters probably sustained for 18-76 days and 4-23 days within the hypoxic centers during the three summer months (June-August), respectively, synonymous with 20.5%-84.5% of low-oxygen occurrences (HF4) and 4.8%-25.2% of hypoxia occurrences (HF3) in summer (Fig. 5j, m; Table 2). As for the 2010s, the estimated thickness of hypoxia in the Modaomen sub-estuary has substantially increased to ~1.5 m, while the low-oxygen thickness in the Hong Kong waters has reached ~5 m (approximately 4 m thicker relative to the 1990s; Fig. 5h). Furthermore, the duration of the low-oxygen and hypoxic events in the 2010s was prolonged, roughly at 55-89 days (61.0%-99.1% of HF4) and 19-51 days (21.4%-56.5% of HF3) in the hypoxic centers (Fig. 5k, n; Table 2), respectively.

3.2.2 Variations in bottom oxygen consumption

To further explore the mechanism of long-term deoxygenation off the PRE, we investigated the oxygen consumption rates and their changes during the two periods

https://doi.org/10.5194/egusphere-2024-4013
Preprint. Discussion started: 9 January 2025

(the 1990s versus the 2020s). We specifically focused on the oxygen consumption at the bottom layers covering the 20% of the water depth above the sediments, where the majority of hypoxic events in the PRE occurred (Fig. 5).

As shown in Table 2, the predominant oxygen sink in the bottom waters of the PRE was sediment oxygen demand (SOD) induced largely by the remineralization of organic matter in sediments, whereas water column respiration (WCR) only accounted for 15.2% of the bottom oxygen consumption on average. Over the past three decades, both the WCR and SOD have generally enhanced in the PRE, primarily attributed to the growth in local production of organic matter associated with aggravated eutrophication (Fig. 3j-o). Particularly, the SOD in the outer Lingdingyang Bay and Hong Kong waters has remarkably increased from 0.28-0.92 mg O_2 L^{-1} day^{-1} in the 1990s to 1.12-1.48 mg O_2 L^{-1} day^{-1} in the 2010s (Table 2), which contributed to 80%~95% of the increment in total oxygen consumption. Although the absolute increase of SOD in the Modaomen sub-estuary was comparatively small, the SOD in the 2010s has almost doubled compared to the 1990s, leading to a substantial increase in the occurrence of hypoxic events in this region (Fig. 5d-o).

3.2.3 Disentangling contributions of riverine oxygen, suspended sediments, and nutrient changes on deoxygenation

As detailed in Section 2.3, three scenario simulations were performed to quantify the relative contributions of riverine changes to the decadal low-oxygen expansion in the PRE (Table 1). In general, the riverine impacts on DO and related biogeochemical factors varied significantly between subregions (Figs. 6-7). Specifically, increasing the riverine nutrient levels from the 1990s to the 2020s alone (High-nutrient case) led to a marked drawdown in the bottom DO around the lower PRE (by over 0.2 mg/L relative to the 1990s; Fig. 6a). The DO decline, extending from the Modaomen sub-estuary to the Hong Kong waters, was ascribed to the elevated phytoplankton biomass (Fig. 7b) facilitated by better nutrient conditions, which subsequently sustained stronger bottom oxygen depletions compared to the 1990s (Fig. 7c). Among the subregions, the Hong

https://doi.org/10.5194/egusphere-2024-4013
Preprint. Discussion started: 9 January 2025

Kong waters was more susceptible to the changes in riverine nutrients as it was subject to comparatively severe nutrient limitation (Table 2). Therefore, with the improvement of nutrient utilization, this region experienced more pronounced deoxygenation in association with significant alterations in Chl *a* content and SOD (increased by 14.2 μg/m^2 and 0.26 mg O_2 L^{-1} day^{-1}, respectively, equivalent to 47.1% and 46.4% of their total increments over the past three decades; Fig. 7). While in the inner Lingdingyang Bay, the increased nutrient inputs only caused a slight change in Chl *a* content because the phytoplankton growth in this region was mostly light limited due to high water turbidity (Table 2). The concomitant changes in SOD and bottom DO were fairly small as well. Collectively, the high-nutrient scenario alone resulted in a 31% and 34% growth in the area affected by low oxygen (HA4) and hypoxia (HA3) relative to the 1990s, respectively (Table 3).

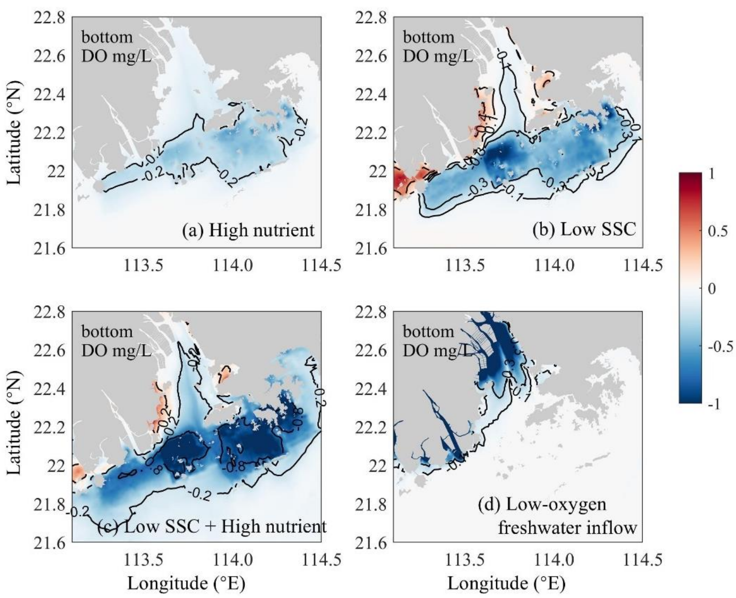

Fig. 6. Bottom DO changes induced by (a) riverine nutrient increases (the High-nutrient case minus the 1990s case), (b) riverine SSC declines (the Low-SSC case minus the 1990s case), (c) the combined effects of nutrient increases and SSC declines (the DO-restore case minus the 1990s case), and (d) riverine DO declines (the DO-restore case minus the 2010s case), respectively.

https://doi.org/10.5194/egusphere-2024-4013
Preprint. Discussion started: 9 January 2025

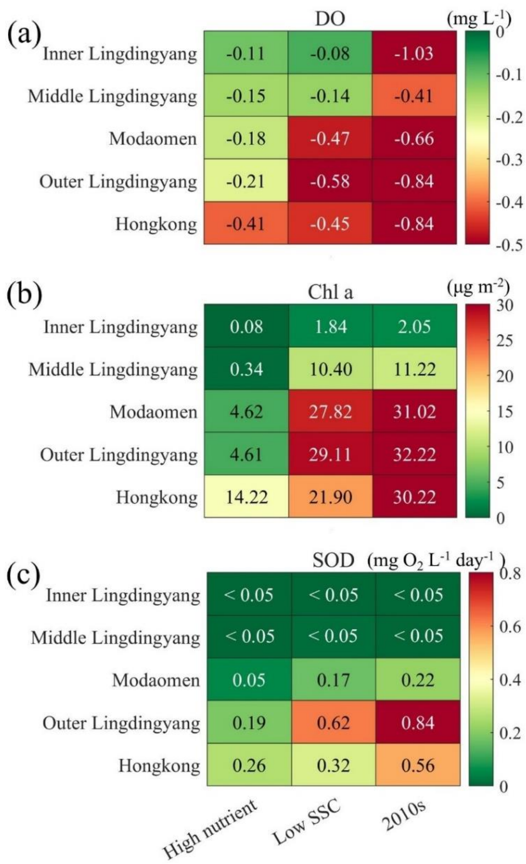

Fig. 7. Changes of (a) bottom DO concentration, (b) vertically-integrated Chl *a* content, and (c) SOD in subregions of the PRE for the High-nutrient, the Low-SSC, and the 2010s cases relative to the 1990s case.

Compared with the High-nutrient case, reducing the riverine suspended sediment loads from the 1990s to the 2020s alone (Low-SSC case) imposed a greater impact on the DO conditions, causing more extensive and intense deoxygenation through the PRE (Fig. 6b). Apparent DO decline (exceeding 0.3 mg/L relative to the 1990s) occurred within the lower PRE, similar to that of the changing riverine nutrients described above. This is also attributed to the intensified SOD (with an increment of 0.17-0.62 mg O_2 L^{-1} day^{-1}, accounting for 57.1%-77.3% of the total increment during the two periods; Fig. 7c), accompanied by a prominent increase in Chl *a* content (by 21.9-29.1 μg/m^2,

https://doi.org/10.5194/egusphere-2024-4013
Preprint. Discussion started: 9 January 2025

accounting for 72.4%-90.3% of the total increment; Fig. 7b) due to the improved light condition (the relief of light limitation; Table 2). The SSC-induced changes in these biogeochemical factors were more pronounced in the outer Lingdingyang Bay and Modaomen sub-estuary than in other regions including the Hong Kong waters, which coincided with the alterations in deoxygenation among the subregions (Fig. 7). Overall, under the low-SSC scenario the low-oxygen area (HA4) and hypoxic area (HA3) expanded by 47% and 95% compared to the 1990s, respectively (Table 3). In addition, it is important to note that the low-SSC-induced exacerbation could be further escalated by superimposing with the effect of high nutrient inputs (Fig. 6c). As shown, the combined actions of decreasing SSC and increasing nutrients (DO-restore case) promoted a larger area of bottom waters off the lower PRE to develop into a low oxygen or hypoxic state, yielding a substantial expansion of low-oxygen conditions (reaching 2409.7 km^2 of HA4 and 617.2 km^2 of HA3; Table 3) that eventually exceeded the sum of changes induced by individual riverine input.

With respect to the influence of altered riverine DO influx, it could be deduced from the difference between the 2010s and the DO-restore cases (Fig. 6d). There was a considerable DO decrease (by over 0.8 mg/L) in the bottom waters adjacent to the river outlets (also in the surface waters) owing to the low-oxygen inflows from the upstream river channels. The impact of these low-oxygen waters was largely restricted within the upper Lingdingyang Bay under the effects of air-sea reoxygenation and water-column mixing along with the river plume transport. Collectively, reducing the riverine DO content from the 1990s to the 2020s alone resulted in an enlargement of low-oxygen area by nearly 515.8 km^2 (derived by subtracting the HA4 of the 2010s case from that of the DO-restore case; Table 3).

4. Discussion

4.1 Impacts of decadal changes in riverine inputs on deoxygenation off the PRE

By combining the long-term observations with simulations from the physical-biogeochemical coupled model, we have elucidated the subsurface deoxygenation and associated mechanisms driven by changes in a variety of riverine inputs over the past three decades in a typical eutrophic estuarine system, namely the Pearl River Estuary (PRE). With the rapid socio-economic development, the inorganic nitrogen and phosphorus contents flowing into the PRE during summer have approximately increased by 100% and 225% from the historical period (1990s) to the present period (2020s), respectively (Table 1). Also, the riverine SSC has decreased by ~60%, consequent to the intense human activities such as dam construction (Liu et al., 2022) and reforestation (Cao et al., 2023). Besides, the amplified oxygen depletion fueled by terrestrial pollutants discharged into the upstream rivers has led to a lower riverine DO concentration (dropped by 46%) entering the estuary (Ma et al., 2024). These alterations have jointly triggered more extensive and persistent low-oxygen conditions in the bottom waters of the PRE (Fig. 5). Based on our model estimation, the summertime low-oxygen (DO < 4 mg/L) and hypoxic (DO < 3 mg/L) areas in the PRE have risen by 148% and 192% during the two periods, respectively (Table 3), together with a significant increase in the vertical thickness (expanding upwards by ~1-4 m) and the duration (extending by ~15-35 days during June-August) of low-oxygen events.

More interestingly, the PRE has developed three distinct hypoxic centers (including the inner Lingdingyang Bay, Modaomen sub-estuary, and Hong Kong waters) controlled by different dominant factors, which renders the deoxygenation problem in this region as a great reference for estuaries and coastal systems worldwide. Specifically, the impact of riverine low-oxygen waters was confined within the upper estuary close to the river outlets, leading to a ~44% increase in the low-oxygen area relative to the 1990s. Such local low-oxygen issue could be mitigated to a large extent if the riverine

https://doi.org/10.5194/egusphere-2024-4013
Preprint. Discussion started: 9 January 2025

DO recovered to a comparatively higher level (e.g., ~6.5 mg/L in the 1990s) according to the DO-restore scenario (Fig. 6d). By comparison, the deoxygenation in the lower estuary primarily followed the classic eutrophication-driven paradigm. As indicated in the High-nutrient and the Low-SSC cases, the increased nutrient inputs and declined suspended sediment loads have separately alleviated the nutrient and light limitations on algae growth in the region, thereby stimulating phytoplankton blooms and local production of organic matter to support subsurface oxygen consumption (dominated by sediment oxygen uptake, SOD; Fig. 7). Our results also indicated that the riverine SSC reduction played a more important role in driving the long-term low-oxygen expansion in the PRE. Its synergistic effect with the riverine nutrient changes could further amplify the exacerbation of eutrophication and subsequent deoxygenation, resulting in an enlarged growth in the low-oxygen area (by 104%) and hypoxic area (by 192%) that was notably larger than the total of their partial contributions (Table 3).

It is worth mentioning that the relative importance of the riverine nutrient and SSC changes were different between the two hypoxic centers in the lower PRE, depending upon their distances from the river outlets. Closer to the river outlets, the Modaomen sub-estuary and its surrounding waters (located on the western side of the coastal transition zone off the PRE) possessed a fairly high SSC level, which imposed a stronger light limitation on the growth of phytoplankton in the region, ultimately making the oxygen dynamics more susceptible to the decline in riverine SSC. On the contrary, the Hong Kong waters and adjacent coastal areas (located on the eastern side of the coastal transition zone) far from the river outlets were less affected by the riverine inputs, where the relatively low nutrient levels promoted more sensitive responses of biogeochemical processes (e.g. primary production and SOD) and hypoxia occurrences to nutrient variations.

4.2 Nutrient control and hypoxia mitigation in the context of sediment declines

Our results underscored the substantial spatial variability in the regulation of riverine inputs on deoxygenation, which implies the necessity for establishing more refined and targeted strategies for hypoxia mitigation. Compared with the riverine nutrients, the influences of SSC on eutrophication and hypoxia have received less attention. It follows that there might be overestimations of the nutrient impacts in the previous studies without considering SSC to ensure the model simulation aligning with the observed deoxygenation. Such an overfitting problem could further lead to an optimistic assessment on the hypoxic mitigation effect under a certain nutrient control plan. Therefore, it is imperative to disentangle or re-evaluate the contribution of riverine nutrients and SSC to the coastal deoxygenation over the past decades. As exemplified in our study for the PRE, a more stringent nutrient reduction might be required to curb the deoxygenation issue given the low SSC status at present.

Furthermore, it should be noted that although the dam constructions in the Pearl River Basin have mostly completed since the 2000s, it is still unclear whether the declining trend of riverine SSC will persist in the future. For instance, the reforestation in recent years has shown to be effective in reducing the summer freshwater discharges and sediment loads in the Pearl River Basin (Cao et al., 2023). Therefore, the role of riverine SSC variations remains critical for oxygen dynamics in the future, which poses greater challenges and uncertainties for eutrophication and hypoxia mitigation. Similar problems also exist in other estuaries and coastal systems suffering hypoxia. For example, it was reported that the decrease of riverine SSC (by ~56%) appeared to be the predominated factor for the intensifying eutrophication (with a 61% increase in the Chl *a* concentration) in the Yangtze River Estuary over the past decades (Wang et al., 2019). In addition, several modelling studies have showed that the dam constructions in the upper regions of Guadiana Estuary have significantly reduced the water turbidity and exacerbated eutrophication in the lower estuary (Domingues et al., 2012; Barbosa et al., 2010). A global-scale survey revealed that the sediment loads in 414 major rivers has approximately decreased by 51% since the 2000s due to human activities (Dethier et al., 2022), suggesting that the deteriorating eutrophication and deoxygenation in the context of sediment declines has become a global concern and merits more attention and investigations in the future.

Some caveats to our work require further studies. For example, apart from anthropogenic activities, alterations in regional physical conditions aligning with climate changes could also regulate the long-term deoxygenation in coastal regions (Chen et al., 2024). The impacts of ocean warming on deoxygenation (Laurent et al., 2018) remain unclear in the PRE as well. While these factors have not been considered in this study, the relative contributions of human activities and climate changes represent a significant topic for future investigations, which can facilitate a more comprehensive understanding of oxygen dynamics and hypoxia development in estuaries and coastal systems.

5. Conclusion

We applied a well-validated physical-biogeochemical model to reconstruct the summertime oxygen distributions in the PRE during two representative periods (the 1990s and the 2010s) and to disentangle the contribution of alterations in riverine inputs (i.e., suspended sediments, nutrients, and oxygen concentration) to the long-term deoxygenation off the PRE based on a suite of model experiments. We found that owing to the changes of riverine inputs over the past three decades, the low-oxygen and hypoxic areas in the bottom waters of the PRE have expanded by about 1.5 times and two-fold, respectively, with the duration time prolonged by ~15-35 days in summer. Concurrently, three hypoxic centers dominated by distinct factors were identified. Scenario simulations revealed that the decline in riverine oxygen concentration has caused a low-oxygen expansion (by ~44%) in the upper PRE. By comparison, the

https://doi.org/10.5194/egusphere-2024-4013
Preprint. Discussion started: 9 January 2025

alterations in riverine nutrients and suspended sediments have separately provided better nutrient and light conditions to promote higher production of labile organic matter, which jointly maintained considerable oxygen depletions and exacerbated the low-oxygen conditions in the lower PRE. The relative importance of the changing riverine nutrients and suspended sediments to deoxygenation varied between subregions. The suspended sediment reduction was the predominated factor in the downstream regions close to the river outlets (e.g. the Modaomen sub-estuary), while the nutrient increase exerted a more substantial influence in the regions far from the river outlets (e.g. the Hong Kong waters). Our study highlights the significant role of the declined suspended sediments in the low-oxygen expansion off the PRE, which can further amplify the effect in association with the increasing nutrients. Therefore, in the context of global regimes changes of riverine suspended sediments, we call for an urgent re-evaluation of the impacts of riverine inputs on deoxygenation in addition to nutrients in order to better understand the mechanism controlling hypoxia and thereby proposing effective mitigation strategies.

CRediT authorship contribution statement

Yue Nan: Investigation, Model experiments, Formal analysis, Visualization, Writing-original draft. **Zheng Chen:** Model experiments, Writing-review. **Bin Wang:** Writing-review. **Bo Liang:** Writing-review. **Jiatang Hu:** Project administration, Supervision, Conceptualization, Writing-review & editing.

Declaration of competing interest

The authors declare that they have no known competing financial interests or personal relationships that could have appeared to influence the work reported in this paper.

Acknowledgements

https://doi.org/10.5194/egusphere-2024-4013
Preprint. Discussion started: 9 January 2025

This work was supported by a grant from the Southern Marine Science and Engineering Guangdong Laboratory (Zhuhai) (Project. SML2023SP220) and two consulting projects (ZB-2023-005, ZB-2023-054) to JH.

Data availability

Data will be made available on request.

https://doi.org/10.5194/egusphere-2024-4013
Preprint. Discussion started: 9 January 2025

Reference

Barbosa, A. B., Domingues, R. B., and Galvão, H. M.: Environmental Forcing of Phytoplankton in a Mediterranean Estuary (Guadiana Estuary, South-western Iberia): A Decadal Study of Anthropogenic and Climatic Influences, Estuaries and Coasts, 33, 324-341, 10.1007/s12237-009-9200-x, 2010.

Bianchi, T. S., DiMarco, S. F., Cowan, J. H., Hetland, R. D., Chapman, P., Day, J. W., and Allison, M. A.: The science of hypoxia in the Northern Gulf of Mexico: A review, Science of The Total Environment, 408, 1471-1484, https://doi.org/10.1016/j.scitotenv.2009.11.047, 2010.

Breitburg, D., Levin, L. A., Oschlies, A., Grégoire, M., Chavez, F. P., Conley, D. J., Garçon, V., Gilbert, D., Gutiérrez, D., Isensee, K., Jacinto, G. S., Limburg, K. E., Montes, I., Naqvi, S. W. A., Pitcher, G. C., Rabalais, N. N., Roman, M. R., Rose, K. A., Seibel, B. A., Telszewski, M., Yasuhara, M., and Zhang, J.: Declining oxygen in the global ocean and coastal waters, Science, 359, eaam7240, 10.1126/science.aam7240, 2018.

Cao, Z., Duan, H., Ma, R., Shen, M., and Yang, H.: Remarkable effects of greening watershed on reducing suspended sediment flux in China's major rivers, Science Bulletin, 68, 2285-2288, 2023.

Carstensen, J., Andersen, J. H., Gustafsson, B. G., and Conley, D. J.: Deoxygenation of the Baltic Sea during the last century, Proceedings of the National Academy of Sciences of the United States of America, 111, 5628-5633, 10.1073/pnas.1323156111, 2014.

Chen, J. Y., Pan, D. L., Liu, M. L., Mao, Z. H., Zhu, Q. K., Chen, N. H., Zhang, X. Y., and Tao, B. Y.: Relationships Between Long-Term Trend of Satellite-Derived Chlorophyll-a and Hypoxia Off the Changjiang Estuary, ESTUARIES AND COASTS, 40, 1055-1065, 10.1007/s12237-016-0203-0, 2017.

Chen, L., Zhang, X., He, B., Liu, J., Lu, Y., Liu, H., Dai, M., Gan, J., and Kao, S.-J.: Dark Ammonium Transformations in the Pearl River Estuary During Summer, Journal of Geophysical Research: Biogeosciences, 125, e2019JG005596, https://doi.org/10.1029/2019JG005596, 2020.

Chen, Z., Yu, L., and Hu, J.: Disentangling the contributions of anthropogenic nutrient input and physical forcing to long-term deoxygenation off the Pearl River Estuary, China, Water Research, 265, 122258, https://doi.org/10.1016/j.watres.2024.122258, 2024.

Cullen, J. J.: Subsurface Chlorophyll Maximum Layers: Enduring Enigma or Mystery Solved?, in: ANNUAL REVIEW OF MARINE SCIENCE, VOL 7, edited by: Carlson, C. A., and Giovannoni, S. J., 207-239, 10.1146/annurev-marine-010213-135111, 2015.

Dethier, E. N., Renshaw, C. E., and Magilligan, F. J.: Rapid changes to global river suspended sediment flux by humans, Science, 376, 1447-1452, 10.1126/science.abn7980, 2022.

Diaz, R. J. and Rosenberg, R.: Spreading dead zones and consequences for marine ecosystems, Science, 321, 926-929, 10.1126/science.1156401, 2008.

Domingues, R. B., Barbosa, A. B., Sommer, U., and Galvão, H. M.: Phytoplankton composition, growth and production in the Guadiana estuary (SW Iberia): Unraveling changes induced after dam construction, Science of The Total Environment, 416, 300-313, https://doi.org/10.1016/j.scitotenv.2011.11.043, 2012.

Fizpartick, J.: A user's guide for RCA (release 3.0), HydroQual Inc., New Jersey, USA. 217p, 2004.

Ge, J., Torres, R., Chen, C., Liu, J., Xu, Y., Bellerby, R., Shen, F., Bruggeman, J., and Ding, P.: Influence of suspended sediment front on nutrients and phytoplankton dynamics off the Changjiang Estuary: A FVCOM-ERSEM coupled model experiment, Journal of Marine Systems, 204, 103292, https://doi.org/10.1016/j.jmarsys.2019.103292, 2020.

Hu, J. and Li, S.: Modeling the mass fluxes and transformations of nutrients in the Pearl River Delta, China, Journal of Marine Systems, 78, 146-167, https://doi.org/10.1016/j.jmarsys.2009.05.001, 2009.

Hu, J., Li, S., and Geng, B.: Modeling the mass flux budgets of water and suspended sediments for the river network and estuary in the Pearl River Delta, China, Journal of Marine Systems, 88, 252-266, https://doi.org/10.1016/j.jmarsys.2011.05.002, 2011.

Hu, J., Zhang, Z., Wang, B., and Huang, J.: Long-term spatiotemporal variations in and expansion of low-oxygen conditions in the Pearl River estuary: a study synthesizing observations during 1976–2017, Biogeosciences, 18, 5247-5264, 10.5194/bg-18-5247-2021, 2021.

Huang, Y.-G., Yang, H.-F., Jia, J.-J., Li, P., Zhang, W.-X., Wang, Y. P., Ding, Y.-F., Dai, Z.-J., Shi, B.-W., and Yang, S.-L.: Declines in suspended sediment concentration and their geomorphological and biological impacts in the Yangtze River Estuary and adjacent sea, Estuarine, Coastal and Shelf Science, 265, 107708, https://doi.org/10.1016/j.ecss.2021.107708, 2022.

Lai, Y., Jia, Z., Xie, Z., Li, S., and Hu, J.: Water quality changes and shift in mechanisms controlling hypoxia in response to pollutant load reductions: A case study for Shiziyang Bay, Southern China, Science of The Total Environment, 842, 156774, https://doi.org/10.1016/j.scitotenv.2022.156774, 2022.

Laurent, A., Fennel, K., Ko, D. S., and Lehrter, J.: Climate change projected to exacerbate impacts of coastal eutrophication in the northern Gulf of Mexico, Journal of Geophysical Research: Oceans, 123, 3408-3426, 2018.

Li, D., Gan, J., Hui, R., Liu, Z., Yu, L., Lu, Z., and Dai, M.: Vortex and Biogeochemical Dynamics for the Hypoxia Formation Within the Coastal Transition Zone off the Pearl River Estuary, Journal of Geophysical Research: Oceans, 125, 10.1029/2020jc016178, 2020a.

Li, D., Gan, J., Hui, C., Yu, L., Liu, Z., Lu, Z., Kao, S.-j., and Dai, M.: Spatiotemporal Development and Dissipation of Hypoxia Induced by Variable Wind-Driven Shelf Circulation off the Pearl River Estuary: Observational and Modeling Studies, Journal of Geophysical Research: Oceans, 126, e2020JC016700, https://doi.org/10.1029/2020JC016700, 2021.

https://doi.org/10.5194/egusphere-2024-4013
Preprint. Discussion started: 9 January 2025

Li, G., Liu, J., Diao, Z., Jiang, X., Li, J., Ke, Z., Shen, P., Ren, L., Huang, L., and Tan, Y.: Subsurface low dissolved oxygen occurred at fresh- and saline-water intersection of the Pearl River estuary during the summer period, Marine Pollution Bulletin, 126, 585-591, 10.1016/j.marpolbul.2017.09.061, 2018.

Li, X., Lu, C., Zhang, Y., Zhao, H., Wang, J., Liu, H., and Yin, K.: Low dissolved oxygen in the Pearl River estuary in summer: Long-term spatio-temporal patterns, trends, and regulating factors, Marine Pollution Bulletin, 151, 110814, https://doi.org/10.1016/j.marpolbul.2019.110814, 2020b.

Liu, Z., Fagherazzi, S., Liu, X., Shao, D., Miao, C., Cai, Y., Hou, C., Liu, Y., Li, X., and Cui, B.: Long-term variations in water discharge and sediment load of the Pearl River Estuary: Implications for sustainable development of the Greater Bay Area, Frontiers in Marine Science, 9, 983517, 10.3389/fmars.2022.983517, 2022.

Lu, Z., Gan, J., Dai, M., Liu, H., and Zhao, X.: Joint Effects of Extrinsic Biophysical Fluxes and Intrinsic Hydrodynamics on the Formation of Hypoxia West off the Pearl River Estuary, Journal of Geophysical Research: Oceans, 123, 6241-6259, 10.1029/2018jc014199, 2018.

Luo, X., Yang, Q., and Jia, L.: The Riverbed Evolution of the River-Network System in the Pearl River Delta, Sun Yat-sen Univeristy Press, Guangzhou, China, 2002.

Ma, C., Zhao, J., Ai, B., Sun, S., and Yang, Z.: Machine Learning Based Long-Term Water Quality in the Turbid Pearl River Estuary, China, Journal of Geophysical Research: Oceans, 127, e2021JC018017, https://doi.org/10.1029/2021JC018017, 2022.

Ma, R., Chen, Z., Wang, B., Xu, C., Jia, Z., Li, L., and Hu, J.: Spatiotemporal variations and controlling mechanism of low dissolved oxygen in a highly urbanized complex river system, Journal of Hydrology: Regional Studies, 52, 101691, https://doi.org/10.1016/j.ejrh.2024.101691, 2024.

Murphy, R. R., Kemp, W. M., and Ball, W. P.: Long-Term Trends in Chesapeake Bay Seasonal Hypoxia, Stratification, and Nutrient Loading, ESTUARIES AND COASTS, 34, 1293-1309, 10.1007/s12237-011-9413-7, 2011.

Pitcher, G. C., Aguirre-Velarde, A., Breitburg, D., Cardich, J., Carstensen, J., Conley, D. J., Dewitte, B., Engel, A., Espinoza-Morriberón, D., Flores, G., Garçon, V., Graco, M., Grégoire, M., Gutiérrez, D., Hernandez-Ayon, J. M., Huang, H.-H. M., Isensee, K., Jacinto, M. E., Levin, L., Lorenzo, A., Machu, E., Merma, L., Montes, I., Swa, N., Paulmier, A., Roman, M., Rose, K., Hood, R., Rabalais, N. N., Salvanes, A. G. V., Salvatteci, R., Sánchez, S., Sifeddine, A., Tall, A. W., Plas, A. K. v. d., Yasuhara, M., Zhang, J., and Zhu, Z. Y.: System controls of coastal and open ocean oxygen depletion, Progress in Oceanography, 197, 102613, https://doi.org/10.1016/j.pocean.2021.102613, 2021.

Roman, M. R., Brandt, S. B., Houde, E. D., and Pierson, J. J.: Interactive effects of Hypoxia and temperature on coastal pelagic zooplankton and fish, Frontiers in Marine Science, 6, 10.3389/fmars.2019.00139, 2019.

Su, J., Dai, M., He, B., Wang, L., Gan, J., Guo, X., Zhao, H., and Yu, F.: Tracing the origin of the oxygen-consuming organic matter in the hypoxic zone in a large eutrophic

https://doi.org/10.5194/egusphere-2024-4013
Preprint. Discussion started: 9 January 2025

estuary: the lower reach of the Pearl River Estuary, China, Biogeosciences, 14, 4085-4099, 10.5194/bg-14-4085-2017, 2017.

Wang, B., Hu, J., Li, S., and Liu, D.: A numerical analysis of biogeochemical controls with physical modulation on hypoxia during summer in the Pearl River estuary, Biogeosciences, 14, 2979-2999, 10.5194/bg-14-2979-2017, 2017.

Wang, B., Hu, J., Li, S., Yu, L., and Huang, J.: Impacts of anthropogenic inputs on hypoxia and oxygen dynamics in the Pearl River estuary, Biogeosciences, 15, 6105-6125, 10.5194/bg-15-6105-2018, 2018.

Wang, H., Dai, M., Liu, J., Kao, S.-J., Zhang, C., Cai, W.-J., Wang, G., Qian, W., Zhao, M., and Sun, Z.: Eutrophication-Driven Hypoxia in the East China Sea off the Changjiang Estuary, Environmental Science & Technology, 50, 2255-2263, 10.1021/acs.est.5b06211, 2016.

Wang, J. J., Bouwman, A. F., Liu, X. C., Beusen, A. H. W., Van Dingenen, R., Dentener, F., Yao, Y. L., Glibert, P. M., Ran, X. B., Yao, Q. Z., Xu, B. C., Yu, R. C., Middelburg, J. J., and Yu, Z. G.: Harmful Algal Blooms in Chinese Coastal Waters Will Persist Due to Perturbed Nutrient Ratios, ENVIRONMENTAL SCIENCE & TECHNOLOGY LETTERS, 8, 276-284, 10.1021/acs.estlett.1c00012, 2021.

Wang, K., Chen, J., Jin, H., Li, H., Gao, S., Xu, J., Lu, Y., Huang, D., Hao, Q., and Weng, H.: Summer nutrient dynamics and biological carbon uptake rate in the Changjiang River plume inferred using a three end-member mixing model, Continental Shelf Research, 91, 192-200, https://doi.org/10.1016/j.csr.2014.09.013, 2014.

Wang, Y., Wu, H., Lin, J., Zhu, J., Zhang, W., and Li, C.: Phytoplankton Blooms off a High Turbidity Estuary: A Case Study in the Changjiang River Estuary, Journal of Geophysical Research: Oceans, 124, 8036-8059, 10.1029/2019jc015343, 2019.

Wen, G., Liang, Z., Xu, X., Cao, R., Wan, Q., Ji, G., Lin, W., Wang, J., Yang, J., and Huang, T.: Inactivation of fungal spores in water using ozone: Kinetics, influencing factors and mechanisms, Water Research, 185, 116218, https://doi.org/10.1016/j.watres.2020.116218, 2020.

Wu, C. S., Yang, S., Huang, S., and Mu, J.: Delta changes in the Pearl River estuary and its response to human activities (1954–2008), Quaternary International, 392, 147-154, https://doi.org/10.1016/j.quaint.2015.04.009, 2016.

Zhang, H. and Li, S.: A numerical study on hypoxia and primary production in the Pearl River Estuary in summer using the modified RCA water quality model, Journal of tropical oceanography, 29, 2010.

Zhang, Z., Wang, B., Li, S., Huang, J., and Hu, J.: On the Intra-annual Variation of Dissolved Oxygen Dynamics and Hypoxia Development in the Pearl River Estuary, Estuaries and Coasts, 45, 1305-1323, 10.1007/s12237-021-01022-0, 2022.